

GEODESIC COMPLEXITY OF MOTION PLANNING

DAVID RECIO-MITTER

ABSTRACT. We introduce the geodesic complexity of a metric space, inspired by the topological complexity of a topological space. Both of them are numerical invariants, but, while the TC only depends on the homotopy type, the GC is an invariant under isometries. We show that in some cases they coincide but we also develop tools to distinguish the two in a range of examples. To this end, we study what we denote the total cut locus, which does not appear to have been explicitly considered in the literature.

To the knowledge of the author, the GC is a new invariant of a metric space. Furthermore, just like the TC, the GC has potential applications to the field of robotics.

1. INTRODUCTION

Almost two decades ago Farber introduced the topological complexity of a space to study the motion planning problem from robotics using topological tools [7]. In short, the topological complexity is the smallest number of continuous rules necessary to motion plan on a given space, where a motion planning rule is a function which associates to each pair of points a path between them. Fewer rules signify higher stability (continuity) with respect to the input (pairs of points), which is why we seek to minimize the number of such rules.

To give the formal definition the following is needed: The *free path fibration* is the evaluation map $PX \rightarrow X \times X$ which sends each path γ to the pair $(\gamma(0), \gamma(1))$.

Definition 1.1 (Farber '03). The *topological complexity* $TC(X)$ of a space X is defined to be the smallest k for which there exists a decomposition into Euclidean Neighbourhood Retracts (ENRs) $X \times X = \bigsqcup_{i=0}^k E_i$ such that there are local sections $s_i: E_i \rightarrow PX$ of the free path fibration.

In the last two decades, the topological complexity has been computed for a multitude of different spaces by several authors. Furthermore, other variants of topological complexity have emerged, most of which essentially impose some restrictions on the motion planners. For instance, monoidal topological complexity requires the motion from each point to itself to be the constant path. It is an open question of Iwase and Sakai whether $TC(X) = TC_M(X)$ [11]. The equality has been shown for large classes of spaces [6].

From the point of view of applications, the latter restriction is very sensible: if a robot is already at the position to which it needs to move, it is a waste of energy for the robot to move at all. More generally, it is preferable for the motion planner to assign to each pair of points a path of minimal length between them. This is what motivates the definition of geodesic complexity below. First we need some preliminary definitions.

Date: April 19, 2022.

Definition 1.2. Let (X, d) be a metric space. Let γ be a path in X and let $\ell(\gamma)$ denote its length. We say that γ is a minimal geodesic if $\ell(\gamma) = d(\gamma(0), \gamma(1))$. Note that this is the shortest length a path from $\gamma(0)$ to $\gamma(1)$ could possibly have.

Remark 1.3. It is well known that, in the case when X is a Riemannian manifold, minimal geodesics in the sense of the previous definition need to be geodesics in the usual sense of Riemannian geometry (namely locally length minimizing).

Definition 1.4. Let $GX \subset PX$ be the subspace of the free path space of X consisting of minimal geodesics. Restricting the free path fibration $PX \rightarrow X \times X$ to GX yields a map $\pi: GX \rightarrow X \times X$.

Remark 1.5. The map π is no longer a fibration (except in the very special case when it is a homeomorphism). In section 3 we will see that it is sometimes a branched covering.

Definition 1.6. The *geodesic complexity* of (X, d) , $GC(X, d)$ is defined to be the smallest k for which there exists a decomposition into $k+1$ ENRs $X \times X = \bigsqcup_{i=0}^k E_i$ such that there are local sections $s_i: E_i \rightarrow GX$ of π . We call such a collection of local sections a *geodesic motion planner* with $k+1$ ENRs.

Remark 1.7. By definition, $TC(X) \leq GC(X, d)$. The topological complexity is a homotopy invariant and so it does not depend on the metric d . We will see that the geodesic complexity does depend on the metric and is in general different from the topological complexity.

The most commonly used definition of topological complexity (which is equivalent for reasonably nice spaces X) requires an open cover instead of a decomposition into ENRs. However, open sets do not work in the case of geodesic complexity; see Remark 3.3.

There already exists a variant of topological complexity in the literature motivated by the idea of requiring the motion planners to be as efficient as possible, introduced by Błaszczuk and Carrasquel-Vera in 2018 [1]:

Definition 1.8 (Błaszczuk–Carrasquel-Vera '18). Let M be a compact orientable Riemannian manifold with Riemannian metric d . The *efficient topological complexity* $\ell TC(M)$ of M is defined to be the smallest k for which there exists a decomposition into locally compact sets $M \times M = \bigsqcup_{i=0}^k G_i$ such that there are local sections $s_i: G_i \rightarrow PM$ of the free path fibration satisfying

$$\int_{M \times M} \ell \circ s_i = \int_{M \times M} d.$$

However, geodesic complexity is in fact very different from efficient topological complexity, despite the similar heuristics: Błaszczuk and Carrasquel-Vera show that $TC(M) \leq \ell TC(M) \leq TC(M) + 1$ for any closed orientable Riemannian manifold. In fact, they pose the (still open, to our knowledge) question of whether the first inequality is actually an equality $TC(M) = \ell TC(M)$ for closed orientable Riemannian manifold¹. By contrast, we show that the difference between the geodesic complexity and the topological complexity is arbitrarily large, even for closed Riemannian manifolds.

¹They do give one example of a manifold with boundary with $TC(M) = 0$ and $\ell TC(M) = 1$, namely a closed hemisphere of the standard 2-sphere

Theorem 1.9. *For every $k \in \mathbb{N}$ exist a Riemannian manifold (M, g) such that $\text{GC}(M) - \text{TC}(M) \geq k$. In fact, M can be chosen to be a sphere (with a non-standard metric).*

In sections 4, 5 and 6 the geodesic complexity of several spaces is computed. It is worth noting that the lower bounds are proven by direct considerations of explicit motion planners (i.e. without recourse to algebra), which is very uncommon in the field of topological complexity and its variants. The ideas used there might be applicable to many further examples. We summarize the findings in the following theorems.

Theorem 1.10 (Theorems 4.4 and 4.5). *For the flat n -torus T^n and the flat Klein bottle K , the topological complexity and the geodesic complexity agree: $\text{GC}(T^n) = \text{TC}(T^n) = n$ and $\text{GC}(K) = \text{TC}(K) = 4$.*

It turns out that the assumption in the last theorem that the torus be equipped with the flat metric is essential:

Theorem 1.11 (Theorem 5.1). *Let T_{emb} be the standard embedded torus in \mathbb{R}^3 and let T be the flat 2-torus. Then*

$$\text{GC}(T_{emb}) = 3 > \text{GC}(T) = 2.$$

Theorem 1.12 (Theorem 6.2). *Let W be the boundary of the 3-cube with the flat metric. This is a 2-sphere with a non-standard metric for which the geodesic complexity is different from the topological complexity:*

$$\text{GC}(W) \geq 3 > \text{TC}(W) = \text{TC}(S^2) = 2.$$

The upper bounds on geodesic complexity in the previous theorems come from explicit geodesic motion planners. In particular, we give an optimal geodesic motion planner for the Klein bottle K . While it was known that a (not necessarily geodesic) motion planner with 5 sets exists by the general dimensional upper bound, no such motion planner had not been constructed explicitly. In particular we give a direct proof of $\text{GC}(K) = 4$, which is arguably much simpler than the proofs of $\text{TC}(K) = 4$, first by Cohen and Vandembroucq in 2018 [3] and later by Iwase, Sakai and Tsutaya [12]. Both proofs involve complicated algebraic calculations. It would be a simplification if one could show that $\text{GC}(K) = \text{TC}(K)$ without any knowledge of $\text{TC}(K)$ and then use the first principles proof of $\text{GC}(K) = 4$ given in this article to show $\text{TC}(K) = 4$. It seems likely that the geodesic complexity and the topological complexity agree on a large class of examples which might include the flat Klein bottle.

The most commonly used upper bound for topological complexity is $\text{TC}(X) \leq \dim(X \times X)$ [7], where $\dim(X \times X)$ is the covering dimension. We were not able to find metric spaces for which we can prove that $\text{GC}(X) > \dim(X \times X)$, which leaves open the possibility that the dimensional upper bound also holds for geodesic complexity. However, there does not seem to be a reason for $\text{GC}(X) \leq \dim(X \times X)$ to hold, since the arguments used in the case of topological complexity do not apply in the geodesic setting.

Question 1: Does the bound $\text{GC}(X) \leq \dim(X \times X)$ hold for sufficiently nice metric spaces X ?

Other commonly used bounds for topological complexity are given by the Lusternik-Schnirelmann category $\text{cat}(X)$, which is the smallest k for which there is an open

cover $X = \bigcup_{i=0}^k U_i$ such that each inclusion $U_i \hookrightarrow X$ is null-homotopic. The Lusternik-Schnirelmann category is a homotopy invariant which is closely related to topological complexity. In [7] Farber shows that:

$$\text{cat}(X) \leq \text{TC}(X) \leq \text{cat}(X \times X)$$

The lower bound trivially carries over to geodesic complexity since $\text{TC}(X) \leq \text{GC}(X)$. However, the upper bound does not carry over: According to Theorem 1.9, there is a Riemannian metric g_m , such that $\text{GC}(S^{n+1}, g_m) \geq n$, while it is well-known that $\text{cat}(S^n \times S^n) = 2$. Furthermore, Theorem 6.2 also yields a counterexample, since the theorem states that $\text{GC}(W) \geq 3$, and yet $\text{cat}(W \times W) = \text{cat}(S^2 \times S^2) = 2$.

Possibly the bound can be recovered by replacing the Lusternik-Schnirelmann category with a geodesic version. Given a metric space X , let $\text{Gcat}(X)$ be the smallest k for which there is an decomposition into ENRs $X = \bigsqcup_{i=0}^k E_i$ such that each $E_i \hookrightarrow X$ is null-homotopic along geodesics (meaning that the homotopy restricted to any point of X yields a geodesic). It is easy to see that $\text{Gcat}(X) \leq \text{GC}(X)$ but the proof of $\text{TC}(X) \leq \text{cat}(X \times X)$ does not carry over to the geodesic case.

Question 2: Does the bound $\text{GC}(X) \leq \text{Gcat}(X \times X)$ hold for sufficiently nice metric spaces X ?

I would like to thank Diarmuid Crowley, Don Davis, Mark Grant, Mike Harrison and Jarek Kędra for very valuable discussions and suggestions.

2. ARE $\text{GC}(X)$ AND $\text{TC}(X)$ EQUAL?

A priori $\text{GC}(X)$ and $\text{TC}(X)$ could actually be the same for reasonable metric spaces X (assuming at least that X is geodesically complete, to make sure that $\text{GC}(X)$ is not automatically infinite). However, in this section we construct Riemannian manifolds M for which the numbers $\text{GC}(M)$ and $\text{TC}(M)$ are arbitrarily far apart from each other. In fact, the constructed manifolds are spheres with non-standard Riemannian metrics.

We need the following definition.

Definition 2.1. A submanifold K of a Riemannian manifold (M, g) is said to be *convex* if for any pair of points $x, y \in K$, every minimal geodesic in M between x and y lies entirely in K .

Theorem 2.2. *If K is a convex submanifold of (M, g) , then $\text{TC}(K) \leq \text{GC}(K, g|_K) \leq \text{GC}(M, g)$.*

Proof. A geodesic motion planner in $M \times M$ obviously restricts to a geodesic motion planner in $K \times K$. \square

We will need the following theorem.

Theorem 2.3 (Farber [7]). *Let S^n be the n -sphere and T^n the n -torus. Then*

$$\text{TC}(S^n) = \begin{cases} 1 & \text{if } n \text{ odd} \\ 2 & \text{if } n \text{ even} \end{cases}$$

and

$$\text{TC}(T^n) = n.$$

The following example will motivate the proof of Theorem 1.9.

Example 2.4. Let (S^3, g_m) be the result of glueing a hemisphere of the standard sphere (S^3, g) onto each end of the standard cylinder $S^2 \times [0, 1]$. This space is sometimes known as a capsule. After smoothing the edges, (S^3, g_m) becomes a Riemannian manifold diffeomorphic to S^3 . Because the submanifold $S^2 \times \{\frac{1}{2}\} \simeq S^2$ is convex, by Theorem 2.2: $\text{GC}(S^3, g_m) \geq \text{TC}(S^2) = 2 > 1 = \text{TC}(S^3)$.

The proof of Theorem 1.9 is essentially a generalization of the previous example.

Proof of Theorem 1.9. Let (S^{n+1}, g) be the standard sphere of radius 1, with $n \geq 2$.

Let $T^n \hookrightarrow S^{n+1}$ be an embedding of a torus with trivial normal bundle. Choose a tubular neighbourhood N_1 of T^n in S^{2n+2} and further tubular neighborhood N_2 around N_1 . Because the normal bundle is trivial, N_1 is homeomorphic to a product $T^n \times (-1, 1)$. Construct a new Riemannian metric g_m on S^{n+1} such that it coincides with g outside of N_2 and it corresponds to the product metric on $N_1 \cong T^n \times (-100, 100)$. It is well known that a metric can be chosen in $N_2 - N_1$ to make (S^{n+1}, g_m) into a Riemannian manifold.

Given two points x and y in $(T^n, g_m|_{T^n})$, all shortest paths between x and y must stay in N_1 because a path leaving N_1 would be much longer than the diameter of $(T^n, g_m|_{T^n})$. Furthermore, because $g_m|_{N_1}$ is the product metric it is clear that the shortest paths all have to lie on $T^n \times \{0\} \subset N_1$. This shows that $(T^n, g_m|_{T^n})$ is convex in (S^{n+1}, g_m) .

By Theorem 2.2 we have $\text{GC}(S^{n+1}, g_m) \geq \text{TC}(T^n) = n$, while $\text{TC}(S^{n+1})$ equals either 1 or 2. The difference $\text{GC}(S^{n+1}, g_m) - \text{TC}(S^{n+1}) \geq n - 2$ can be made arbitrarily large by increasing n . \square

3. THE TOTAL CUT LOCUS AND LOWER BOUNDS FOR GC

Let (X, d) be a metric space. The following definition is very useful when studying $\text{GC}(X)$.

Definition 3.1. The *total cut locus* of X is the subset $C \subset X \times X$ consisting of all pairs (x, y) for which there is more than one minimal geodesic γ from x to y . The *cut locus of a point* $x \in X$ is the subset $C_x \subset X$ consisting of all y in X such that (x, y) is in C .

The cut locus of a point is treated in many differential geometry textbooks, such as [13]. However, the author was not able to find any mention of the total cut locus (by any name) in the literature.

The geodesic complexity seems to depend entirely on the nature of the total cut locus. It is not obvious how to describe this relationship explicitly. However, we study the total cut locus of several examples in sections 4, 5 and 6 to find lower bounds for the geodesic complexity. These examples seem to point to a general method to find lower bounds for the geodesic complexity of a metric space in cases in which the preimages $\pi^{-1}((x, y))$ are finite for all $(x, y) \in X \times X$, using completely different ideas than the ones used in Section 2.

The simplest example in which to present some of the ideas used in sections 4, 5 and 6 is the following.

Example 3.2. Let S^1 be the unit circle with the standard Riemannian metric. The preimage of a pair (x, y) under the map $\pi: GS^1 \rightarrow S^1 \times S^1$ is either a single geodesic (when (x, y) lies outside the total cut locus C) or two geodesics (when (x, y) lies on the total cut locus C). Restricting the map π to C yields a 2-sheeted

covering and restricting the map π to $S^1 \times S^1 - C$ yields a 1-sheeted covering (i.e. a homeomorphism).

The total cut locus C can be visualized as a diagonal circle inside the torus $S^1 \times S^1$. As we noted, there are two sheets over each pair in C . We can approach such a pair from the complement of C from two sides. The map π is the result of gluing a 1-sheeted covering over the complement of C with a 2-sheeted covering over C : The single sheet over $S^1 \times S^1 - C$ converges to a different sheet over C when approaching from a different side.

Furthermore, a local section $s_i: E_i \rightarrow GS^1$ consists of a continuous choice of sheet over each point in E_i . No pair in the total cut locus can lie in the interior of a set E_i because no neighborhood of such a pair admits a continuous choice of sheet. This implies that $\text{GC}(S^1) \geq 1$.

That lower bound also follows from the well known fact $\text{TC}(S^1) = 1$ (see Theorem 2.3). However, this serves as a very simple example of a more general method to get lower bounds for the geodesic complexity of a space.

Finally, $\text{GC}(S^1) = 1$ because there exists an obvious geodesic motion planner with two ENRs $E_0 = S^1 \times S^1 - C$ and $E_1 = C$, which was already constructed by Farber to prove $\text{TC}(S^1) = 1$ [7] (let $s_1((x, y))$ be the minimal geodesic going clockwise).

Remark 3.3. The previous example makes clear that defining geodesic complexity using an open cover (as opposed to a decomposition into ENRs) would not work, given that if a set contains a point of the total cut locus in its interior then it does not admit a local section of π .

As was pointed out in the introduction, the map $\pi: GX \rightarrow X \times X$ is not a fibration. However, if the preimages $\pi^{-1}((x, y))$ are finite for all $(x, y) \in X \times X$ then the map π sometimes is a branched covering in the following sense.

Definition 3.4. A *stratification* of X is a decomposition

$$X = \bigsqcup_{i=1}^k S_i$$

into disjoint subsets, called *strata*, such that $S_i \subset \overline{S_j}$ if and only if $i \geq j$

Let X be a space with a stratification as in the previous definition. Then a branched covering is a map $p: E \rightarrow X$ which satisfies the following:

- (1) Restricting p to each stratum S_i yields a covering.
- (2) The sheets of the covering map $p|_{S_j}$ approach sheets of the covering map $p|_{S_i}$ when $S_i \subset \overline{S_j}$.
- (3) Every sheet of of the covering map $p|_{S_i}$ is in the closure of some sheet of the covering map $p|_{S_j}$ whenever $S_i \subset \overline{S_j}$.

Remark 3.5. It might be useful to place further restrictions to the stratification in the definition above, such as the S_i being manifolds of decreasing dimension.

By understanding how the coverings over the strata are glued together we can give lower bounds for the geodesic complexity. Furthermore, the strata themselves can be used to construct a decomposition into ENRs for an explicit geodesic motion planner, yielding an upper bound for the geodesic complexity. See Example 3.2 and sections 4 and 5.

It is worth noting that in Section 6 we find a lower bound for geodesic complexity using the same ideas but without the need of fully understanding the branched covering structure of π , only some of its local properties.

4. SPACES FOR WHICH $\text{TC}=\text{GC}$

Some of the first spaces for which Farber computed the topological complexity are the spheres, see Theorem 2.3. To prove the optimal upper bound for $\text{TC}(S^n)$ he constructed an explicit motion planner. Because that motion planner is geodesic (for the standard Riemannian metric on the sphere), the upper bound extends to $\text{GC}(S^n)$. Together with the lower bound $\text{TC}(X) \leq \text{GC}(X)$ this yields:

Proposition 4.1. *Let S^n be the standard n -dimensional sphere. The $\text{GC}(S^n) = \text{TC}(S^n)$.*

Not long after the computation of $\text{TC}(S^n)$, Farber, Tabachnikov and Yuzvinsky computed $\text{TC}(\mathbb{R}P^n)$ for all real projective spaces $\mathbb{R}P^n$. The result uncovered a surprising link between topological complexity and the immersion dimension, given in the following theorem. Recall that the immersion dimension $\text{Immdim}(M)$ of a smooth manifold M is the smallest k such that M can be immersed into \mathbb{R}^k .

Theorem 4.2 (Farber–Tabachnikov–Yuzvinsky [9]). *Let $\mathbb{R}P^n$ be the n -dimensional projective space. Then*

$$\text{TC}(\mathbb{R}P^n) = \begin{cases} n & \text{if } n = 1, 3, 7 \\ \text{Immdim}(M) & \text{otherwise} \end{cases}.$$

Farber, Tabachnikov and Yuzvinsky give a motion planner in [9, Theorem 7.3] which realizes the upper bound $\text{TC}(\mathbb{R}P^n) \leq \text{Immdim}(\mathbb{R}P^n)$. While that motion planner is not geodesic, it can be easily modified to become geodesic. The same ideas can be used to give optimal geodesic motion planners in the cases where n equals 1, 3 or 7. Just as in the case of spheres we get:

Proposition 4.3. *Let $\mathbb{R}P^n$ be the standard n -dimensional real projective space. The $\text{GC}(\mathbb{R}P^n) = \text{TC}(\mathbb{R}P^n)$.*

The remainder of this section is devoted to computing the geodesic complexity of Riemannian manifolds, the torus T and the Klein bottle K , both equipped with the flat metric. We will show the lower bounds using the ideas mentioned in Section 3, rather than using $\text{TC}(X) \leq \text{GC}(X)$. In Section 6 we will see that the lower bound coming from this technique can be strictly better than the lower bound $\text{TC}(X) \leq \text{GC}(X)$.

The following theorem shows that $\text{TC}(T^n) = \text{GC}(T^n)$.

Theorem 4.4. *Let T^n be the n -torus equipped with the flat metric. Then $\text{GC}(T^n) = n$.*

Proof. Stratification and upper bound

The n -torus $T^n = (S^1)^n$ as a stratification $(S_k)_{1 \leq k \leq n+1}$ with:

$$S_k = \{(x, y) \in T^n \times T^n \mid y_i = x_i + \pi \text{ for precisely } k - 1 \text{ many } i\}$$

The sets S_k were used in Cohen and Pruidze [2] as ENRs for an explicit motion planner in the torus, which is actually a geodesic motion planner. Note that the minimal geodesics on T^n with the flat metric are the paths in which all coordinates

move simultaneously at constant speed along the shortest arc in the corresponding S^1 factor. If (x, y) is in S_k , there are precisely $k-1$ coordinates which are antipodal. For each of those $k-1$ coordinates we need to choose to move either clockwise or counterclockwise in that coordinate, which results in 2^{k-1} many minimal geodesics between x and y . If we vary (x, y) within S_k the minimal geodesics vary continuously and if we approach S_m from S_k the minimal geodesics over S_k converge to minimal geodesics over S_m . We see that $\pi: GT \rightarrow T \times T$ is a branched covering in the sense of Section 3.

Cohen and Pruidze show in [2, Proposition 3.3] that it is possible to make continuous choices of minimal geodesic over each S_k , yielding a motion planner on $n+1$ sets. This implies the upper bound $\text{GC}(T^n) \leq n$.

Lower bound for $n=2$

The lower bound immediately follows from $\text{GC}(T) \geq \text{TC}(T) = 2$. However, we will prove that $\text{GC}(T) \geq 2$ directly by studying the stratification given above.

We will first give a proof for $n=2$ which can be extended to all n in a straightforward manner. Let $T = T^2$.

Assume, for the sake of contradiction, that we have a decomposition $T \times T = E_0 \sqcup E_1$ with local sections s_0 and s_1 of $\pi: GT \rightarrow T \times T$ over E_0 and E_1 respectively.

Let (x, y) be in S_3 . We may assume that (x, y) is in E_0 . Let U_ϵ be a small ball around y . For the remainder of the proof, the point x will be fixed. Let $\tilde{E}_i = \{y' \in T \mid (x, y') \in E_i\}$.

Note that because $(x, y) \in S_3$ we have $y_1 = x_1 + \pi$ and $y_2 = x_2 + \pi$. We may identify T^2 with the quotient of a square centered around x , in which the corners represent y : $T = [0, 2\pi]^2 / \sim$ with $(0, x_2) \sim (2\pi, x_2)$ and $(x_1, 0) \sim (x_1, 2\pi)$. The four distinct geodesics from x to y (the sheets of the branched covering $GT \rightarrow T \times T$ over (x, y)) can then be characterized by the directions up-right, up-left, down-right and down-left (UR, UL, DR, DL); see Figure 1. By abuse of notation, we will call geodesics which are very close to one of those 4 minimal geodesics by the same name. For example, all geodesics very close to UR will also be denoted UR.

The cut locus C_x of x divides the ball U_ϵ into four open chambers with their boundaries intersecting at y , see Figure 1. The chamber decomposition has a cell structure compatible with the stratification: y is the vertex and (x, y) is in S_3 , if y' is in an edge then (x, y') is in S_2 and if y'' is in the interior of a chamber then (x, y'') is in S_1 .

For points y'' in the interior of a chamber of U_ϵ , the unique minimal geodesic between x and y'' is one of UR, UL, DR, DL, depending on the chamber containing y'' . In this way we can identify the chambers with the minimal geodesics and label them UR, UL, DR, DL just as in Figure 1.

Let y' be on the edge between chambers UR and DR. Assume, for the sake of contradiction, that y' is in the interior of \tilde{E}_0 . Then we would be able to find two sequences $(y_I''^k)$ and $(y_{II}''^k)$ in \tilde{E}_0 converging to y' with $y_I''^k$ in UR and $y_{II}''^k$ in DR. By assumption, we have a local section $s_0: E_0 \rightarrow GT$. By continuity $s_0((x, y_I''^k)) = UR$ and $s_0((x, y_{II}''^k)) = DR$ need to converge to the same path $s_0((x, y'))$, which yields a contradiction. Therefore, no y' cannot lie neither in the interior of \tilde{E}_0 or \tilde{E}_1 . In other words, every y' lying on an edge must be in the closure of both \tilde{E}_0 and \tilde{E}_1 .

Recall that (x, y) is in E_0 . We showed that every point on an edge between chambers lies in the closure of \tilde{E}_0 (and \tilde{E}_1). Using this and a diagonal argument

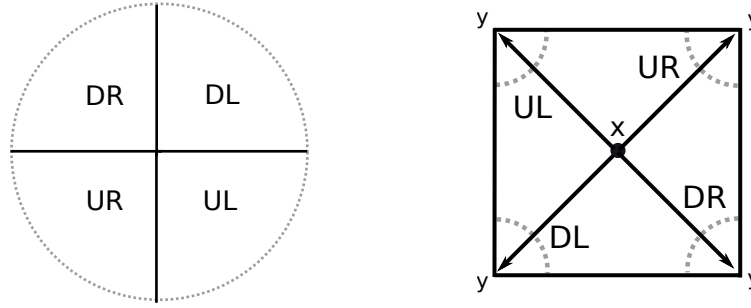


FIGURE 1. The small ball U_ϵ divided into chambers. The second picture is of T^2 , seen as the square with opposite sides identified with each other in the second picture. All the corner points represent the same point in T^2 .

we can construct a sequence (y^{lk}) in \tilde{E}_0 converging to y , such that (y^{lk}) is contained in a small neighbourhood around the edge between the chambers UR and DR, for instance. Note that, by construction, $s_0((x, y^{lk}))$ must then converge to either the geodesic UR or the geodesic DR. By continuity, $s_0((x, y))$ must be either UR or DR.

However, if we assume instead that y' lies on the edge between the chambers UL and DL, the same argument would imply that $s_0((x, y))$ must be either UL or DL. This yields a contradiction.

Lower bound for $n \geq 3$

The lower bound for $n \geq 3$ follows by iterating the argument for the case $n = 2$.

Consider $T^3 = (S^1)^3$, for instance. Let $(x, y) \in S_4 \subset T^3 \times T^3$ and let U_ϵ be a small ball around y . This ball will have a chamber decomposition, just as for $n = 2$, except that the square in Figure 1 has to be replaced by a cube. When $n = 3$ there are eight 3-dimensional open chambers, separated by 2-dimensional walls, which intersect along edges, which in turn all intersect at the vertex at the center of the ball U_ϵ .

Analogously to the case with $n = 2$, we may show that every y'' in a 2-dimensional wall is in the closure of at least two \tilde{E}_i .

Now assume, for the sake of contradiction, that there exists a point y' in an edge which has a neighborhood V_ϵ which is contained in $\tilde{E}_0 \cup \tilde{E}_1$. The point y' can be approached by a sequence (y''^k) contained in $V_\epsilon \cap W$, where W is a wall adjacent to y' . Because each y''^k is on a wall, it is in the closure of at least two \tilde{E}_i . Since each y''^k is in V_ϵ , it must be in the closure of \tilde{E}_0 (and \tilde{E}_1). Using a diagonal argument we may construct a sequence (\tilde{y}''^k) converging to y' contained in W or a chamber adjacent to W and such that (\tilde{y}''^k) is contained in \tilde{E}_0 . By continuity, $s_0((x, \tilde{y}''^k))$ must tend to $s_0((x, y'))$ as k tends to infinity, meaning that $s_0((x, y'))$ is compatible with one of the chambers adjacent to W . However, we could do the same argument with any wall adjacent to y' and deduce that $s_0((x, y'))$ is compatible with a chamber adjacent to every wall. This yields a contradiction because there is no chamber adjacent to every wall. Therefore, every point y' in an edge is in the closure of at least three \tilde{E}_i .

Next we assume, for the sake of contradiction, that the small ball U_ϵ around y is contained in $\tilde{E}_0 \cup \tilde{E}_1 \cup \tilde{E}_2$. The point y can be approached by a sequence (y'^k) contained in $\tilde{E}_0 \cup \tilde{E}_1 \cup \tilde{E}_2$ and on an edge L . Because each y'^k is in the closure of at least three \tilde{E}_i , it is in the closure of \tilde{E}_0 (and \tilde{E}_1 and \tilde{E}_2). Using a diagonal argument we may construct a sequence (\tilde{y}'^k) converging to y contained in L or a chamber adjacent to L and such that (\tilde{y}'^k) is contained in \tilde{E}_0 . By continuity, $s_0((x, \tilde{y}'^k))$ must tend to $s_0((x, y))$ as k tends to infinity, meaning that $s_0((x, y))$ is compatible with one of the chambers adjacent to L . However, we could do the same argument with any edge and deduce that $s_0((x, y'))$ is compatible with a chamber adjacent to every edge. This yields a contradiction because there is no chamber adjacent to every edge. Therefore, the point y is in the closure of at least four \tilde{E}_i . This implies that $\text{GC}(T^3) \geq 3$.

In the case of general n the ball U_ϵ around y is divided into 2^n many n -dimensional chambers separated by $(n-1)$ -dimensional walls going through the center of the ball and meeting along $(n-2)$ -dimensional walls and so on. The k -dimensional walls correspond to the k -skeleton of the n -dimensional cube intersected with small balls around the corner points. By induction on the argument above we can show that every point of a k -dimensional wall needs to be in the closure of $n-k+1$ many \tilde{E}_i , which implies that $\text{GC}(T^n) \geq n$ (seeing the vertex as a 0-dimensional wall). \square

Note that Cohen and Vandembroucq proved that $\text{TC}(K) = 4$. In the following theorem we compute the geodesic complexity of the Klein bottle, without making use of the fact that $\text{GC}(K) \geq \text{TC}(K)$ and thus independently of their result, which is very hard to prove.

The topological complexity of the higher-dimensional Klein bottles K_n (introduced in [4]) is unknown, but an argument similar to the one given in the proof of the theorem, albeit with much more complicated cut loci, yields the geodesic complexity of K_n for all n ; this is done by Davis and the author in [5].

Theorem 4.5. *Let K be the Klein bottle equipped with the flat metric. Then $\text{GC}(K) = 4$.*

Proof. Stratification

The total cut locus of the Klein bottle is somewhat similar to the total cut locus of the torus but more complex. Before going through the following proof it is helpful to first read the proof of the previous theorem.

Let $K = [0, 1]^2 / \sim$ with $(0, x_2) \sim (1, 1 - x_2)$ and $(x_1, 0) \sim (x_1, 1)$.

The total cut locus of the torus is completely homogeneous, in the following sense. If we fix a point x in the torus, then the cut locus at x is homeomorphic to $S^1 \vee S^1$. As we translate x in the torus, the cut locus is simply translated along with x .

In the case of the Klein bottle, the cut locus of a point changes as we move the point around K . To understand the total cut locus of K we will make use of the universal covering $p: \mathbb{R}^2 \rightarrow K$. Given a point x in K , we can determine its cut locus C_x in the following way.

Consider the set of all lifts $p^{-1}(x)$ in \mathbb{R}^2 under the universal covering. Now choose one point in $p^{-1}(x)$ and draw segments between that point and all the other lifts in $p^{-1}(x)$. Then the cut locus C_x is the projection of the convex hull of the bisecting lines of all those segments. In Figure 2 we see that in the case $x_2 = 0$ or

$x_2 = 1/2$ the convex hull is a square which projects to $S^1 \vee S^1 \subset K$, the cut locus of x , just as in the case of the torus. However, when $x_2 \neq 0, 1/2, 1$ the convex hull is a (non-regular) hexagon, which projects down to a θ graph with edges of different lengths; see Figure 3.

After the preliminaries above we are ready to describe how C_x changes as we move x .

If we start moving a point x with $x_2 = 0$ vertically, the cut locus C_x continuously deforms from a wedge $S^1 \vee S^1$ into a θ graph. The smallest edge gradually gets longer while one of the other edges of the graph gets shorter. Once x reaches the other orientation reversing “meridian” (for example we go up from $x_2 = 0$ to $x_2 = 1/2$), the new edge turns into a circle of the cut locus $S^1 \vee S^1$, while the edge that was getting shorter has been contracted into the basepoint.

On the other hand, if we move x horizontally the cut locus is merely translated along.

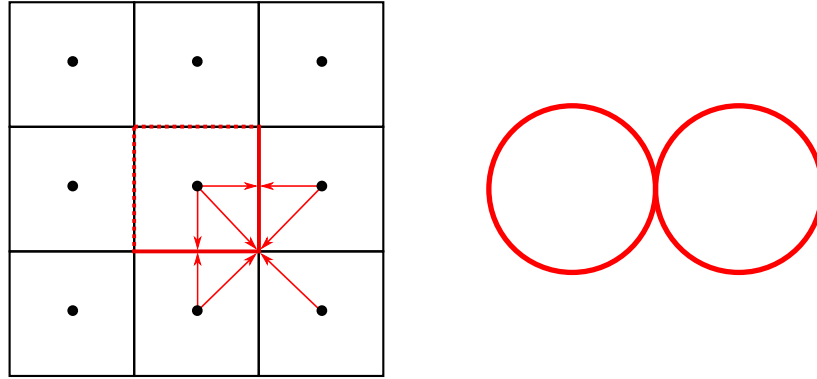


FIGURE 2. The cut locus of the point $(1/2, 1/2)$ in the Klein bottle is a wedge of circles. The picture for the torus is exactly the same in this case.

We construct the following stratification, which shows that $\pi: GK \rightarrow K \times K$ is a branched covering in the sense of Section 3.

- (1) The set S_1 is the complement of the total cut locus. That is, the pairs (x, y) in S_1 are covered by a unique minimal geodesics.
- (2) The set S_2 consists of the pairs (x, y) covered by precisely two minimal geodesics. This is the case precisely when y lies in the interior of one of the edges of C_x , which is either $S^1 \vee S^1$ or a θ graph.
- (3) The set S_3 consists of the pairs (x, y) covered by precisely three minimal geodesics. This is the case precisely when $x_2 \neq 0, 1/2, 1$ and y lies on one of the vertices of the θ graph C_x .
- (4) The set S_4 consists of the pairs (x, y) covered by precisely four minimal geodesics. This is the case precisely when $x_2 = 0, x_2 = 1/2$ or $x_2 = 1$ and y is the vertex of $S^1 \vee S^1 = C_x$.

Upper bound

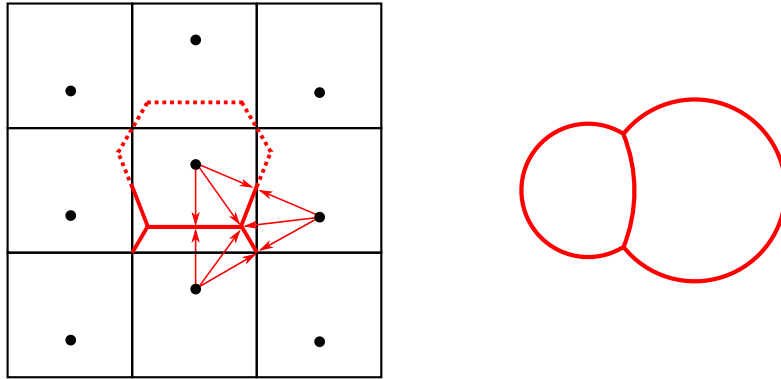


FIGURE 3. The cut locus of points between $(1/2, 1/2)$ and $(1/2, 1)$ in the Klein bottle. When the point moves up from $(1/2, 1/2)$ a new edge appears at the vertex and then it keeps growing, while another edge gets shorter.

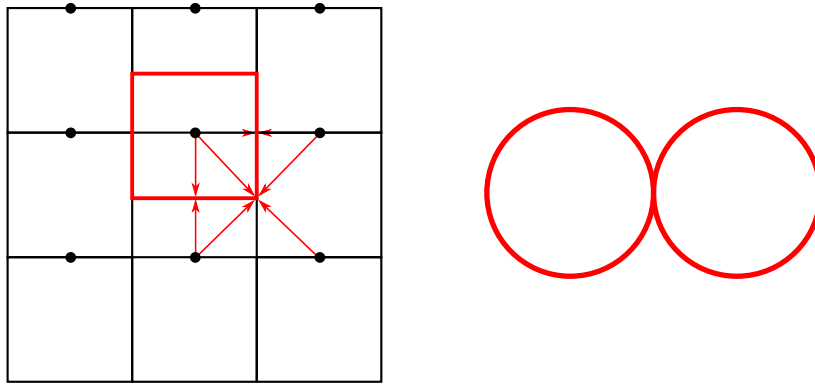


FIGURE 4. The cut locus of the point $(0, 1)$ in the Klein bottle is a wedge of circles again. The new edge that appeared when moving up from $(1/2, 1/2)$ has completely replaced the old vertical edge.

For the upper bound we will construct a geodesic motion planner with 5 sets. That is, a decomposition $K \times K = \bigsqcup_{i=0}^4 E_i$ such that there is a local section of $\pi: GK \rightarrow K \times K$ over each E_i .

Note that there is no local section of $GK \rightarrow K \times K$ on S_i for $i = 2, 3, 4$ because we cannot make a consistent choice of a geodesic going “up” or “down” on the Klein bottle. To get sets E_i with which we can define a geodesic motion planner we can “cut” the strata so as to make it impossible to go once around the Klein bottle along an orientation reversing curve. We are going to divide the pairs (x, y) into two sets, depending on whether x lies in the annulus $A = \{(x_1, x_2) \in K \mid x_1 \neq 0\}$.

We set

$$S_i^A = \{(x, y) \in S_i \mid x \in A\}$$

and $S_i^c = S_i - S_i^A$.

This yields another stratification of $K \times K$:

- (1) $\tilde{E}_0 = S_1$
- (2) $\tilde{E}_1 = S_2^A$
- (3) $\tilde{E}_2 = S_2^c \sqcup S_3^A$
- (4) $\tilde{E}_3 = S_3^c \sqcup S_4^A$
- (5) $\tilde{E}_4 = S_4^c$

Intuitively, the sets range from more to less generic. The disjoint unions above indicate that the sets are topologically disjoint.

We will construct local sections $s_i: E_i \rightarrow GK$ for all i by constructing them separately on every path component of E_i .

The section $s_0: E_0 \rightarrow GK$ simply maps (x, y) to the unique minimal geodesic between x and y .

The set $E_1 = S_2^A$ has three path components. The first path component contains those pairs (x, y) such that x is in the annulus A and y is being represented by a point which is in the interior of the horizontal edges either of the square or of the hexagon in figures 2 and 3. In this case, there are precisely two minimal geodesics between x and y , one going up and one going down, and $s_1((x, y))$ can be chosen to be the geodesic going up. Note that there is a consistent choice of up and down because x has to remain in A . There are two further path components in E_1 , containing those pairs (x, y) such that x is in the annulus A and y is being represented by a point which is in the interior of either the vertical edges of the square in Figure 2 or in the slanted edges of the hexagon in Figure 3. As the coordinate y_2 approaches 0 (or 1) or $1/2$ one of the slanted edges of the hexagon becomes a vertical edge of the square and the other one disappears. Both for vertical edges and slanted edges, there are precisely two minimal geodesics between x and y , one going to the right and one going to the left, and choosing $s_1((x, y))$ to be the geodesic going to the right yields a continuous map.

For the set $E_2 = S_2^c \sqcup S_3^A$ we are going to define the section $s_2: E_2 \rightarrow GK$ separately on S_2^c and S_3^A . For S_2^c the situation is analogous as for S_2^A above, replacing A by its complement (a circle). The set S_3^A consists of pairs (x, y) such that x lies in A and satisfies $x_2 \neq 0$ (and $x_2 \neq 1$) and $x_2 \neq 1/2$, and y lies on one of the two vertices of the θ -graph C_x . In terms of Figure 3, y is being represented by a corner of the hexagon. Note that x is restricted to two disjoint open squares on which the corners of the hexagon remain completely separate. In fact, S_3^A has four path components homeomorphic to $(0, 1)^2$, because for each of the two open squares containing x , y can be one of the two vertices in the θ -graph C_x . For (x, y) on a given path component, there will be precisely three minimal geodesics from x to y , either two going to the left and one to the right, or two going to the right and one to the left. Choosing $s_1((x, y))$ to be the geodesic going to the right in the former case and to the left in the latter case (for instance) yields a continuous map.

For the set $E_3 = S_3^c \sqcup S_4^A$ we are going to define the section $s_3: E_3 \rightarrow GK$ separately on S_3^c and S_4^A . For S_3^c the situation is analogous as for S_3^A above, replacing A by its complement (a circle). For (x, y) in S_4^A there are precisely four minimal geodesics from x to y . This situation corresponds to y being represented by a point which is on a corner of the cube in Figure 2. The set S_4^A has two path components homeomorphic to $(0, 1)$, depending on whether $x_2 = 0$ or $x_2 = 1/2$. We choose the geodesic going up and to the right (represent y by the upper right corner) for each path component.

For the set $E_4 = S_4^c$ the situation is analogous as for S_4^A above, replacing A by its complement (a circle).

The above could be summarized conceptually as follows. The path components of the E_i are either contractible or have the homotopy type of the circle. We have shown that $GK \rightarrow K \times K$ becomes a trivial covering when restricted to each path component, by constructing sections of all those coverings.

Lower bound

For the lower bound we use the stratification S_i .

We want to show $\text{GC}(K) \geq 4$. Assume, for the sake of contradiction, that we have a decomposition $K \times K = \bigsqcup_{i=0}^3 E_i$ such that there exist local sections $s_i: E_i \rightarrow GK$.

Choose a point (x, y) in S_4 and fix it for the remainder of the proof. We may assume that (x, y) is in E_0 .

Now assume, for the sake of contradiction, that there is a small ball W_ϵ around (x, y) which only intersects E_0, E_1 and E_2 . Choose a small ball U_ϵ around y such that $\{x\} \times U_\epsilon$ is in W_ϵ . The ball U_ϵ is divided into 4 chambers precisely like for the torus in the proof of the last theorem (see Figure 1).

Between x and y there are 4 minimal geodesics. Making a local choice of orientation in the vertical direction (choice of up and down) the minimal geodesics can be characterized by the directions up-right, up-left, down-right and down-left (UR, UL, DR, DL). By abuse of notation, we will denote geodesics which are very close to one of those 4 minimal geodesics by the same name. For example geodesics which are very close to UR will also be denoted UR.

For points y'' in the interior of a chamber of U_ϵ , the unique minimal geodesic between x and y'' is one of UR, UL, DR, DL, depending on the chamber containing y'' . In this way we can identify the chambers with the minimal geodesics and label them UR, UL, DR, DL just as in Figure 1.

Now let (x', y') be in $S_3 \cap W_\epsilon$ and let V_ϵ be a small ball around y' such that $\{x'\} \times V_\epsilon$ is in W_ϵ . Similarly to U_ϵ , the ball V_ϵ is divided into chambers corresponding to the minimal geodesics from x' to y' , but into 3 chambers in this case; see Figure 5. Labelling the chambers by the minimal geodesics associated to them as for S_4 above, we end up with 4 kinds of chamber decompositions of a small ball V_ϵ around a point $(x', y') \in S_3 \cap W_\epsilon$:

- (1) {UR,UL,DR}
- (2) {UR,DL,UL}
- (3) {DR,DL,UL}
- (4) {DR,UR,DL}

Analogously to the proof of the last theorem we can show that every given point of S_3 has to be in the closure of at least 3 different E_i .

Because we assumed that W_ϵ only intersects 3 sets E_0, E_1 and E_2 , all 3 of those sets need to accumulate at every point of $W_\epsilon \cap S_3$. In particular, E_0 accumulates at every point of $W_\epsilon \cap S_3$.

As was explained at the beginning of this proof and illustrated in the figures 2, 3 and 4, the stratum S_3 accumulates at the stratum S_4 . In the figures 6 and 7 we see how all 4 different kinds of 3-chamber decompositions for S_3 merge into the 4-chamber decomposition for S_4 which is looks like Figure 1.

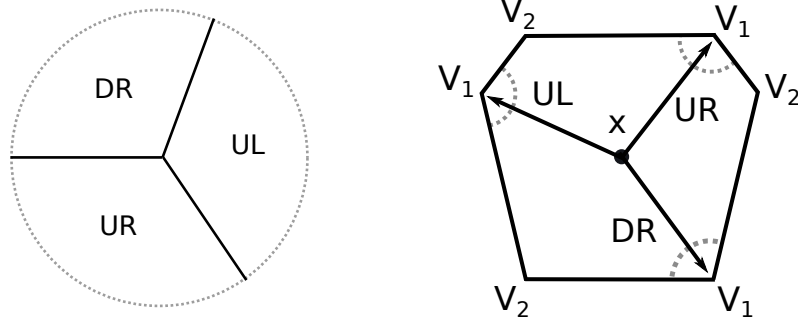


FIGURE 5. The small ball V_ϵ divided into chambers.

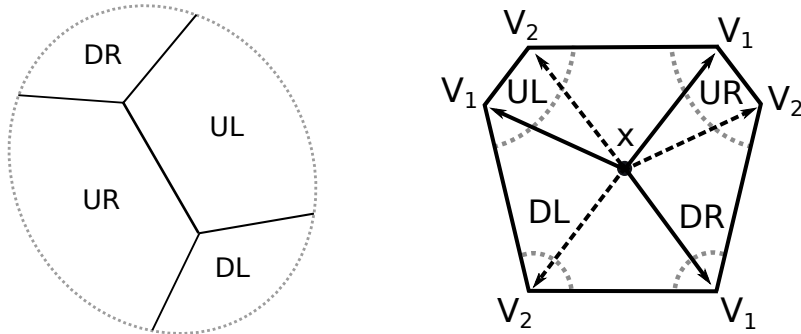


FIGURE 6. As x' approaches x from above the two 3-chamber decompositions around S_3 merge into one 4-chamber decomposition around S_4 , as the hexagon turns into a square.

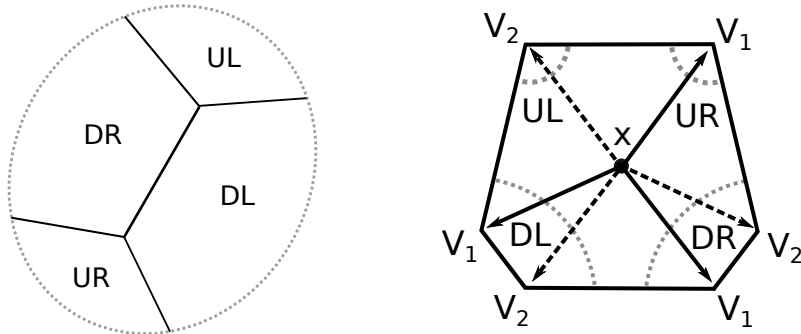


FIGURE 7. As x' approaches x from below the two 3-chamber decompositions around S_3 merge into one 4-chamber decomposition around S_4 , as the hexagon turns into a square.

For instance, there is a sequence of points $((x'^k, y'^k))$ lying in $W_\epsilon \cap S_3$ and converging to (x, y) such that $\pi^{-1}((x'^k, y'^k)) = \{UR, UL, DR\}$ for all k . Using a diagonal argument we can construct another sequence $((x''^k, y''^k))$ in E_0 converging to (x, y) and such that each (x''^k, y''^k) is in a small neighborhood of (x'^k, y'^k) , which implies $\pi^{-1}((x''^k, y''^k)) \in \{UR, UL, DR\}$ for all k . Recall that we abuse notation by

denoting all geodesics which are close to each other by the same name, to simplify the notation. By continuity, $s_0((x''^k, y''^k))$ must converge to $s_0((x, y))$, which means that $s_0((x, y)) \in \{\text{UR, UL, DR}\}$.

However, repeating the argument for the other types of chamber decomposition would imply that $s_0((x, y)) \in \{\text{UR, UL, DR}\} \cap \{\text{UR, DL, UL}\} \cap \{\text{DR, DL, UL}\} \cap \{\text{DR, UR, DL}\} = \emptyset$. This yields a contradiction to our assumption that there is a small ball W_ϵ around (x, y) which only intersects E_0, E_1 and E_2 , which shows that every point of S_4 lies in the closure of at least 4 different E_i .

The above argument is also illustrated slightly differently in Figure 8.

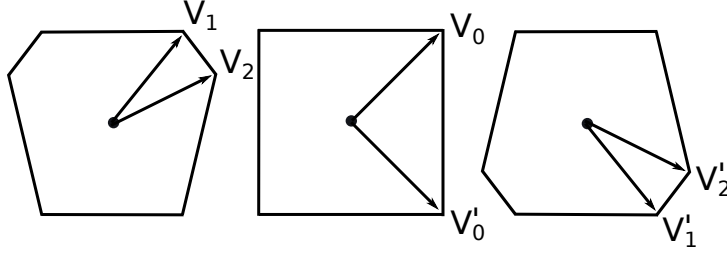


FIGURE 8. As the vertical coordinate x_2 approaches $\frac{1}{2}$, and V_1 (V'_1) and V_2 (V'_2) approach the vertex V_0 (V'_0), the only continuous choice of minimal geodesics requires all geodesics go up (down) when x_2 is approaching $\frac{1}{2}$ from the above (below).

In the final part of the proof we use the assumption that the E_i are ENRs to improve the bound from $\text{GC}(K) \geq 3$ to $\text{GC}(K) \geq 4$. In fact, we only need the E_i to be locally closed for the following argument to work. It is worth noting that this is the only part of the paper where this assumption is used. We have chosen to use ENRs rather than locally closed sets mainly because the ENR definition is very common for topological complexity.

Assume, for the sake of contradiction, that we have a decomposition $X \times X = \bigsqcup_{i=0}^3 E_i$ such that there exist local sections $s_i: E_i \rightarrow GX$. As we showed in part 1, every point of S_4 lies in the closure of at least 4 E_i . Because we are assuming that there are only 4 E_i in the decomposition, S_4 must lie in the closure of every E_i .

Because the E_i are ENRs, they have to be locally closed, which means that they are open in their closure. In particular the intersections $E_i \cap S_4$ yield a decomposition of S_4 into disjoint open sets. This implies that if E_i intersects any point of S_4 , it contains the entire path component of S_4 containing that point. However, no path component of S_4 admits continuous section because there is no consistent choice of up or down, due to the non-orientability of K .

This yields a contradiction, implying that $\text{GC}(K) \geq 4$. \square

5. EMBEDDED TORUS

In this section we prove that the geodesic complexity of the torus embedded in \mathbb{R}^3 in the standard way is higher than the geodesic complexity of the flat torus.

Specifically, the standard embedded torus T_{emb} in \mathbb{R}^3 is given by

$$T_{emb} = \left\{ (x, y, z) \in \mathbb{R}^3 \mid \left(\sqrt{x^2 + y^2} - 2 \right)^2 + z^2 = 1 \right\}.$$

Theorem 5.1. *Let T_{emb} be the embedded torus defined above and let T be the flat 2-torus. Then*

$$GC(T_{emb}) = 3 > GC(T) = 2.$$

Proof. The equality $GC(T) = 2$ follows from Theorem 4.4.

To compute $GC(T_{emb})$ we use the description of the cut locus of any point in T_{emb} given by Gravesen, Markvorsen, Sinclair and Tanaka in [10]:

The cut locus of a point $p = (x_0, 0, z_0)$ with $x_0 > 0$ on the torus is the union of

- (i) the opposite meridian $y = 0, x < 0$,
- (ii) a (piecewise C^1) Jordan curve which intersects the opposite meridian at a single point and is freely homotopic to each parallel, (see Figure 1 in Section 5 of [10]) and, if p is sufficiently far from the inner equator, i.e., if $x_0 > c_2$ for some positive constant c_2 ($> R - r = 2 - 1 = 1$),
- (iii) a pair of subarcs of the parallel $z = -z_0$, each with a conjugate point of p as one endpoint and joining
 - only the Jordan curve of (ii) if $c_2 < x_0 < c_1$ for some c_1 , (see Figure 2 in Section 5 of [10])
 - both of the above if $x_0 = c_1$ (see Figure 3 in Section 5 of [10]) or
 - only the meridian of (i) if $c_1 < x_0$, (see Figure 4 in Section 5 of [10]) at their other endpoint.

In particular, the cut locus of any point in T_{emb} is a graph. Let v_0 denote the vertex at the intersection between the opposite meridian and the parallel $z = -z_0$ in the cut locus of a point $p = (x_0, 0, z_0)$ as described above.

In Figure 9 we illustrate the three different types of cut locus of a point p , in a neighborhood of v_0 .

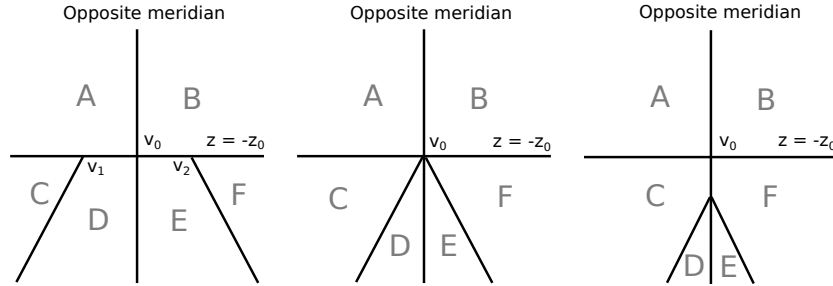


FIGURE 9. The three diagrams represent a neighborhood of the intersection point of the parallel $z = -z_0$ and the opposite meridian in the cut locus of a point $p = (x_0, 0, z_0)$. The value of x_0 increases from the left to the right.

Lower bound

Assume, for the sake of contradiction, that we have a decomposition $T_{emb} \times T_{emb} = \bigsqcup_{i=0}^2 E_i$ such that there exist local sections $s_i: E_i \rightarrow GT_{emb}$.

Let p be a point in T_{emb} and q be a vertex (of degree at least 3) in the cut locus of p . Analogously to the proofs of theorems 4.4 and 4.5 we can show that each such pair (p, q) lies in the closure of E_0 , E_1 and E_2 . We may assume that (p, v_0) is in E_0 .

Let v_1 and v_2 be vertices of the cut locus of a point p as in Figure 9. As the x coordinate of p increases the vertices v_1 and v_2 merge together with v_0 .

There are three minimal geodesics between p and v_1 , each going through one of the three domains A, C and D. Similarly, there are three minimal geodesics between p and v_2 , each going through one of the three domains B, E and F. As we vary p and v_1 and v_2 converge to v_0 , the minimal geodesics $s_0((p, v_1))$ and $s_0((p, v_2))$ need to converge to the same minimal geodesic $s_0((p, v_0))$. However, that is impossible, since the minimal geodesic $s_0((p, v_0))$ would have to go through the a domain contained in $\{A, C, D\} \cap \{B, E, F\} = \emptyset$.

Upper bound

There exists a geodesic motion planner on T_{emb} with the following sets E_i .

- Let E_0 be the complement of the total cut locus of T_{emb} .
- Let E_1 consist of those pairs (p, q) such that q lies in the interior of an edge of the cut locus C_p .
- Let E_2 consist of those pairs (p, q) such that q lies on a vertex of the cut locus C_p other than the vertex v_0 . Recall that v_0 is the intersection point between the meridian and the Jordan curve.
- Let E_3 consist of the pairs (p, v_0) .

There are two minimal geodesics between any pair in E_1 , three minimal geodesics between any pair in E_2 and either four or six minimal geodesics between any pair in E_3 .

Using the description of the cut locus given above that we can make a continuous choice of minimal geodesic over each of the sets E_i , just as for the Klein bottle in the proof of Theorem 4.5. See also the figures in [10, Section 5]. \square

6. FLAT SPHERES

In Section 2 we constructed a Riemannian metric on n -spheres with which the geodesic complexity is strictly greater than the topological complexity. The method used in that section does not work for the 2-sphere, however. It only works for $n \geq 3$ because it relies on having an embedded $n - 1$ -dimensional submanifold M with $\text{TC}(M) > \text{TC}(S^n)$. For $n = 2$ we have that $\text{TC}(S^2) = 2$ and $\text{TC}(M) \leq 2\dim(M) = 2$.

In this section we exhibit a metric on the 2-sphere which yields a higher geodesic complexity than that of the standard 2-sphere. This metric space was provided by Jarek Kędra as an example with a pathological total cut locus when the author was trying to get a better intuition about the cut locus of general metric spaces.

Note that the ideas used in the proof are completely different from the method of Section 2. Instead, we are using the same ideas as for the flat torus and the flat Klein bottle in Section 4 and for the embedded torus in Section 5.

Definition 6.1. Let W be the boundary of the 3-cube with the flat metric. The flat metric comes from identifying W with a subset of the plane with the edges glued together appropriately (see Figure 10). This is a topological manifold which is homeomorphic to the 2-sphere. We call it the flat 2-sphere.

The following theorem is somewhat surprising. Unlike for the spheres in Section 2, we did not construct the metric purposefully to get a higher geodesic complexity in this case.

Theorem 6.2. *Let W be the flat 2-sphere. Then $\text{GC}(W) \geq 3 > 2 = \text{TC}(W)$.*

Remark 6.3. While the 2-sphere W is not smooth, the theorem might still hold after slightly smoothing the edges and corners. The proof seems to carry over to that case, intuitively. However, explicitly describing the geodesics on such a space would require methods from differential geometry.

Proof. The fact that $\text{TC}(W) = \text{TC}(S^2) = 2$ follows from Theorem 2.3 and the homotopy invariance of topological complexity.

The total cut locus of W is quite complicated. However, just as in the previous section, the argument relies on understanding the different minimal geodesics between points arbitrarily close to a specific pair of points. Concretely, in this case it suffices to consider the neighbourhood of a pair of opposite corners in $W \times W$.

Let (x, y) be a pair of points with x and y on opposite faces. Consider the coordinates (x_1, x_2) and (y_1, y_2) for opposite faces given in Figure 10, in which the midpoints of each face acts as the origin and the squares have side length 1.

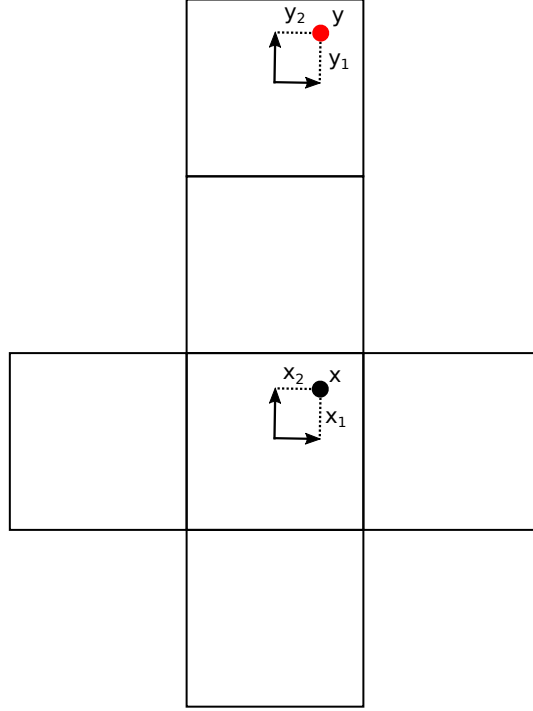


FIGURE 10. We introduce coordinates for points x and y on opposite faces.

As seen in Figure 11, there are at most 12 paths A_1, A_2, \dots, A_{12} which could potentially be minimal geodesics between x and y .

Denoting the length of the path A_i by L_i , we have the following.

- $L_1^2 = (x_1 - y_1)^2 + (2 - x_2 + y_2)^2$
- $L_2^2 = (1 - x_1 + y_2)^2 + (2 - x_2 - y_1)^2$
- $L_3^2 = (1 - x_2 - y_1)^2 + (2 - x_1 + y_2)^2$
- $L_4^2 = (x_2 + y_2)^2 + (2 - x_1 - y_1)^2$

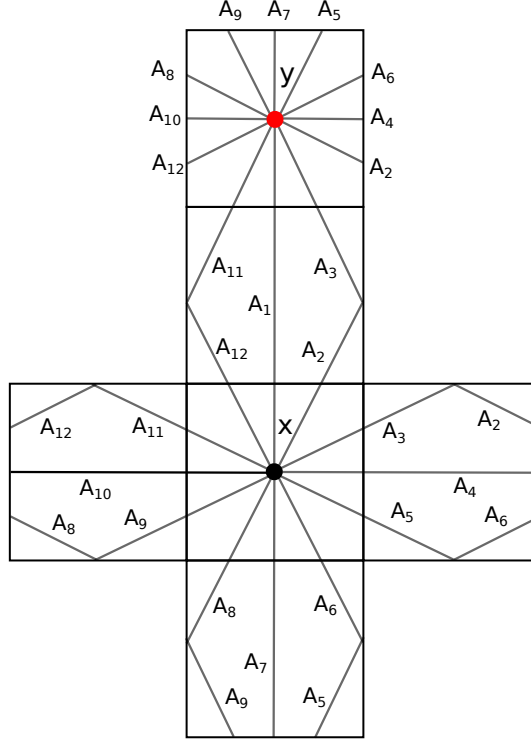


FIGURE 11. There are 12 paths A_1, \dots, A_{12} which are *potentially* minimal geodesics between two points on opposite faces, depending on the specific positions of the points. The points x and y can be anywhere on the two faces. They are in the midpoints of the faces to make the picture more symmetric.

- $L_5^2 = (1 + x_2 - y_1)^2 + (2 - x_1 - y_2)^2$
- $L_6^2 = (1 - x_1 - y_2)^2 + (2 + x_2 - y_1)^2$
- $L_7^2 = (x_1 - y_1)^2 + (2 + x_2 - y_2)^2$
- $L_8^2 = (1 + x_1 - y_2)^2 + (2 + x_2 + y_1)^2$
- $L_9^2 = (1 + x_2 + y_1)^2 + (2 + x_1 - y_2)^2$
- $L_{10}^2 = (x_2 + y_2)^2 + (2 + x_1 + y_1)^2$
- $L_{11}^2 = (1 - x_2 + y_1)^2 + (2 + x_1 + y_2)^2$
- $L_{12}^2 = (1 + x_1 + y_2)^2 + (2 - x_2 + y_1)^2$

It can be readily seen that all the L_i^2 have a common summand $x_1^2 + x_2^2 + y_1^2 + y_2^2$ once we multiply the squares out. Once we subtract that common summand, all expressions have a common factor of 2. To better compare the lengths L_i we will consider the “normalized” square lengths $N_i = (L_i^2 - (x_1^2 + x_2^2 + y_1^2 + y_2^2))/2$:

- $N_1 = -x_1y_1 - 2x_2 + 2y_2 - x_2y_2$
- $N_2 = \frac{1}{2} - x_1 + y_2 - x_1y_2 - 2x_2 - 2y_1 + x_2y_1$
- $N_3 = \frac{1}{2} - x_2 - y_1 + x_2y_1 - 2x_1 + 2y_2 - x_1y_2$
- $N_4 = x_2y_2 - 2x_1 - 2y_1 + x_1y_1$
- $N_5 = \frac{1}{2} + x_2 - y_1 - x_2y_1 - 2x_1 - 2y_2 + x_1y_2$
- $N_6 = \frac{1}{2} - x_1 - y_2 + x_1y_2 + 2x_2 - 2y_1 - x_2y_1$

- $N_7 = -x_1y_1 + 2x_2 - 2y_2 - x_2y_2$
- $N_8 = \frac{1}{2} + x_1 - y_2 - x_1y_2 + 2x_2 + 2y_1 + x_2y_1$
- $N_9 = \frac{1}{2} + x_2 + y_1 + x_2y_1 + 2x_1 - 2y_2 - x_1y_2$
- $N_{10} = x_2y_2 + 2x_1 + 2y_1 + x_1y_1$
- $N_{11} = \frac{1}{2} - x_2 + y_1 - x_2y_1 + 2x_1 + 2y_2 + x_1y_2$
- $N_{12} = \frac{1}{2} + x_1 + y_2 + x_1y_2 - 2x_2 + 2y_1 - x_2y_1$

Now we want to consider two points moving towards a pair of opposite corners p and q with coordinates $p_1 = p_2 = -1/2$ and $q_1 = -q_2 = 1/2$, along the diagonals of opposite faces; see Figure 12. The diagonals are given by $x_1 = x_2$ and $y_1 = -y_2$. For convenience we introduce new coordinates $x_d = -x_1 = -x_2$ and $y_d = y_1 = -y_2$ to describe pairs of points on the diagonals. Because we are going to consider points close to the corners p and q we will limit ourselves to the case $0 < x_d, y_d < 1/2$.

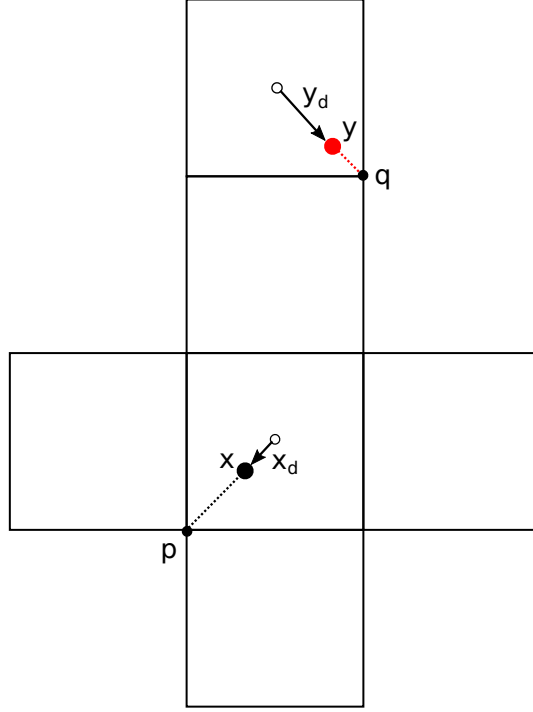


FIGURE 12. We introduce coordinates for points on opposite faces approaching the corner along the diagonal on the respective face.

Assuming that $x_d = -x_1 = -x_2$ and $y_d = y_1 = -y_2$, the normalized lengths above turn into the following expressions (substitute $x_1 = -x_d$, $x_2 = -x_d$, $y_1 = y_d$ and $x_2 = -y_d$).

- $N_1 = 2(x_d - y_d)$
- $N_2 = \frac{1}{2} + 3(x_d - y_d) - 2x_dy_d$
- $N_3 = \frac{1}{2} + 3(x_d - y_d) - 2x_dy_d$
- $N_4 = 2(x_d - y_d)$
- $N_5 = \frac{1}{2} + x_d + y_d + 2x_dy_d$
- $N_6 = \frac{1}{2} - x_d - y_d + 2x_dy_d$

- $N_7 = -2(x_d - y_d)$
- $N_8 = \frac{1}{2} - 3(x_d - y_d) - 2x_d y_d$
- $N_9 = \frac{1}{2} - 3(x_d - y_d) - 2x_d y_d$
- $N_{10} = -2(x_d - y_d)$
- $N_{11} = \frac{1}{2} - x_d - y_d + 2x_d y_d$
- $N_{12} = \frac{1}{2} + x_d + y_d + 2x_d y_d$

If we further assume that the points are at the same distance from the corners (approaching the corners at the same rate) and set $z = x_d = y_d$ (see Figure 13) the expressions simplify further:

- $N_1 = 0$
- $N_2 = \frac{1}{2} - 2z^2$
- $N_3 = \frac{1}{2} - 2z^2$
- $N_4 = 0$
- $N_5 = \frac{1}{2} + 2z + 2z^2$
- $N_6 = \frac{1}{2} - 2z + 2z^2$
- $N_7 = 0$
- $N_8 = \frac{1}{2} - 2z^2$
- $N_9 = \frac{1}{2} - 2z^2$
- $N_{10} = 0$
- $N_{11} = \frac{1}{2} - 2z + 2z^2$
- $N_{12} = \frac{1}{2} + 2z + 2z^2$

Note that N_1, N_4, N_7 and N_{10} are equal and smaller than all other N_i when $-x_1 = y_1 = -x_2 = -y_2 = z$, since all the other N_i are positive, as long as $0 < z < \frac{1}{2}$.

Because the N_i vary continuously, there is a small neighborhood around every pair (x, y) with $0 < -x_1 = y_1 = -x_2 = -y_2 = z < \frac{1}{2}$ in which N_1, N_4, N_7 and N_{10} are shorter than all other N_i . Let U_A be the union of all such neighborhoods. Assuming that (x, y) is in U_A , to determine all the minimal geodesics between x and y we can immediately disregard all paths except A_1, A_4, A_7 and A_{10} .

Note that for pairs (x, y) with $0 < -x_1 = y_1 = -x_2 = -y_2 = z < \frac{1}{2}$ all 4 paths A_1, A_4, A_7 and A_{10} all have the same length, which means that such pairs have exactly 4 preimages under $\pi: GW \rightarrow W \times W$. Therefore, we can construct a sequence (s_A^i) converging to (p, q) with coordinates

$$s_A^i = \left(\left(-\frac{1}{2} + \frac{1}{5i}, -\frac{1}{2} + \frac{1}{5i} \right), \left(\frac{1}{2} - \frac{1}{5i}, -\frac{1}{2} + \frac{1}{5i} \right) \right),$$

such that $\pi^{-1}(s_A^i) = \{A_1, A_4, A_7, A_{10}\}$.

Furthermore, for every sequence component s_A^i we may construct two sequences (r_{iI}^j) and (r_{iII}^j) converging to s_A^i with coordinates

$$r_{iI}^j = \left(\left(-\frac{1}{2} + \frac{1}{5i} + \frac{1}{5j}, -\frac{1}{2} + \frac{1}{5i} + \frac{1}{5j} \right), \left(\frac{1}{2} - \frac{1}{5i}, -\frac{1}{2} + \frac{1}{5i} \right) \right)$$

and

$$r_{iII}^j = \left(\left(-\frac{1}{2} + \frac{1}{5i} - \frac{1}{5j}, -\frac{1}{2} + \frac{1}{5i} - \frac{1}{5j} \right), \left(\frac{1}{2} - \frac{1}{5i}, -\frac{1}{2} + \frac{1}{5i} \right) \right),$$

such that $\pi^{-1}(r_{iI}^j) = \{A_1, A_4\}$ and $\pi^{-1}(r_{iII}^j) = \{A_7, A_{10}\}$.

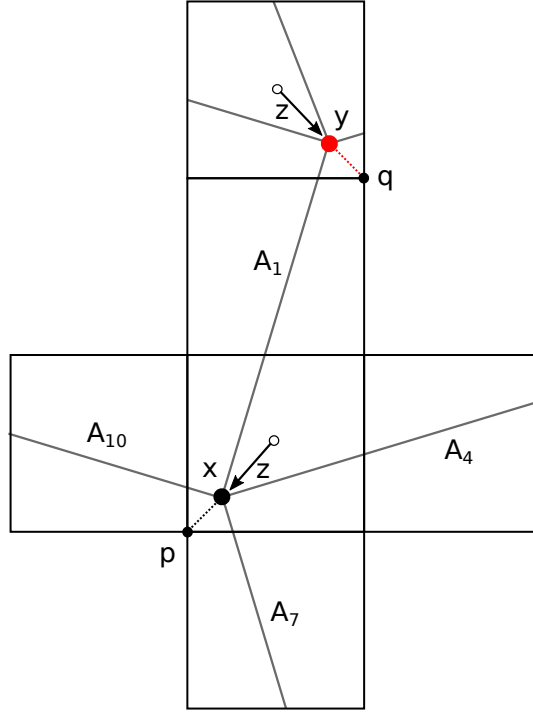


FIGURE 13. We introduce one coordinate z for points on opposite faces approaching the corner along the diagonal on the respective face such that they are always at the same distance from the corners. There are precisely 4 minimal geodesics for such pairs of points.

Finally, for every sequence component r_{iI}^j we can construct two sequences (t_{ijI}^k) and (t_{ijII}^k) converging to r_{iI}^j such that $\pi^{-1}(t_{ijI}^k) = \{A_1\}$ and $\pi^{-1}(t_{ijII}^k) = \{A_4\}$, and similarly for (r_{iII}^j) . To see this note that moving the first point of the pair r_{iI}^j slightly in the direction of the path A_1 results in a pair with unique minimal geodesic A_1 and similarly for A_4 .

Assume, for the sake of contradiction, that we have a decomposition into disjoint ENRs $W \times W = \bigsqcup_{i=0}^2 E_i$ with a local section of $\pi: GW \rightarrow W \times W$ over each E_i .

First we show that all components of the sequences (r_{iI}^j) and (r_{iII}^j) are in the closure of 2 E_i . Assume that there exists a sequence component r_{iI}^j which is in the interior of E_0 , for instance. Then we may assume that (t_{ijI}^k) and (t_{ijII}^k) are in E_0 by taking a subsequence if necessary. By continuity, this would imply that $s_0(t_{ijI}^k) = A_1$ and $s_0(t_{ijII}^k) = A_4$ need to both converge to the same path $s_0(r_{iI}^j)$ as k tends to infinity. This yields a contradiction, implying that every r_{iI}^j lies in the closure of 2 E_i . The same argument applies to (r_{iII}^j) .

Next we show that all components of the sequence (s_A^i) are in the closure of 3 E_i . Assume that there exists a sequence component s_A^i which has a neighborhood V_ϵ which is fully contained in $E_0 \cup E_1$, for instance. We may assume that the sequences (r_{iI}^j) and (r_{iII}^j) are contained in V_ϵ . We showed that all components of

the sequences (r_{iI}^j) and (r_{iII}^j) are in the closure of 2 E_i . Because we assumed that $V_\epsilon \subset E_0 \cup E_1$, this means that every r_{iI}^j and r_{iII}^j lies in the closure of E_0 (and E_1). By a diagonal argument we can construct two new sequences (\tilde{r}_{iI}^j) and (\tilde{r}_{iII}^j) converging to s_A^i which are contained in E_0 , and such that $\pi^{-1}(\tilde{r}_{iI}^j) \in \{A_1, A_4\}$ and $\pi^{-1}(\tilde{r}_{iII}^j) \in \{A_7, A_{10}\}$. This is because pairs sufficiently close to r_{iI}^j and r_{iII}^j cannot have other A_i as minimal geodesics, since the length of the A_i varies continuously. By continuity, this would imply that $s_0(\tilde{r}_{iI}^j) \in \{A_1, A_4\}$ and $s_0(\tilde{r}_{iII}^j) \in \{A_7, A_{10}\}$ need to both converge to the same path $s_0(s_A^i)$ as j tends to infinity. This yields a contradiction, implying that every s_A^i lies in the closure 3 E_i .

Finally, it just remains to show that the pair (p, q) of opposite corners needs to be in the closure of 4 E_i , yielding a contradiction to the existence of the decomposition into 3 E_i above.

There are two other faces adjacent to the corner p , denoted B and C in Figure 14. By using the 3-fold rotation symmetry of the cube around the corners p and q we can construct a neighborhood U_B within which the shortest paths are B_1, B_4, B_7 and B_{10} and a neighborhood U_C within which the shortest paths are C_1, C_4, C_7 and C_{10} , as well as a sequence (s_B^i) converging to (p, q) , such that $\pi^{-1}(s_B^i) = \{B_1, B_4, B_7, B_{10}\}$ and a sequence (s_C^i) converging to (p, q) , such that $\pi^{-1}(s_C^i) = \{C_1, C_4, C_7, C_{10}\}$. Here the paths B_i and C_i are the result of rotating A_i around the axis going through p and q , and similarly for $U_B, U_C, (s_B^i)$ and (s_C^i) .

There are precisely 6 minimal geodesics between p and q as seen in Figure 14. We denote them $D_i, 1 \leq i \leq 6$, just as in the figure. The D_i are limits of the paths A_i, B_i and C_i as pairs of points in U_A, U_B and U_C approach (p, q) . Specifically:

- The paths A_1, A_4, A_7 and A_{10} converge to D_3, D_4, D_6 and D_1 respectively.
- The paths B_1, B_4, B_7 and B_{10} converge to D_5, D_6, D_2 and D_3 respectively.
- The paths C_1, C_4, C_7 and C_{10} converge to D_1, D_2, D_4 and D_5 respectively.

Just as we did above for s_A^i , we can show that all s_B^i and all s_C^i lie in the closure of E_0 (and of E_1 and E_2). Just as above, this allows us to use a diagonal argument to construct new sequences $(\tilde{s}_A^i), (\tilde{s}_B^i)$ and (\tilde{s}_C^i) contained in E_0 and converging to (p, q) such that $\pi^{-1}(\tilde{s}_A^i) \in \{A_1, A_4, A_7, A_{10}\}, \pi^{-1}(\tilde{s}_B^i) \in \{B_1, B_4, B_7, B_{10}\}$ and $\pi^{-1}(\tilde{s}_C^i) \in \{C_1, C_4, C_7, C_{10}\}$.

By continuity, we need $s_0(\tilde{s}_A^i), s_0(\tilde{s}_B^i)$ and $s_0(\tilde{s}_C^i)$ to converge to the same path $s_0((p, q))$. This would imply $s_0((p, q)) \in \{D_3, D_4, D_6, D_1\} \cap \{D_5, D_6, D_2, D_3\} \cap \{D_1, D_2, D_4, D_5\} = \emptyset$, which yields a contradiction. \square

Remark 6.4. We showed that A_1, A_4, A_7 and A_{10} are shorter than the other A_i in a small neighborhood, but it seems plausible that they are shorter for all pairs of points in the *interior* of opposite faces. However, that would require significantly more work to show and we do not need it for this argument. Nonetheless, it would be very interesting to understand the total cut locus and it seems likely that this would allow us to construct a geodesic motion planner with 4 sets, which would show $\text{GC}(W) = 3$.

The map $GW \rightarrow W \times W$ seems to yield a branched covering over a stratified space just as made explicit for the torus and the Klein bottle but it is quite complicated to write down the whole total cut locus.

Remark 6.5. Presumably for the n -dimensional analogues W^n of W the geodesic complexity is $n + 1$, while the topological complexity oscillates between 1 and 2.

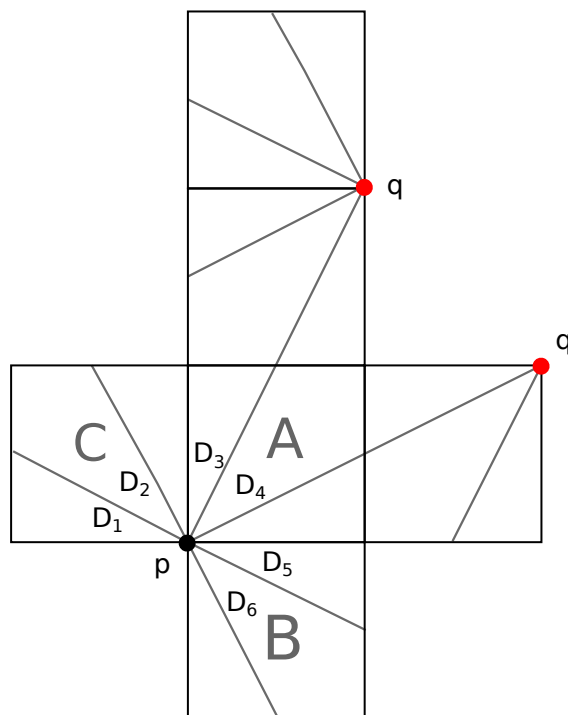


FIGURE 14. There are precisely 6 minimal geodesics between opposite corners p and q . We denote the faces adjacent to p by A , B and C .

If this could be shown, it would yield another (maybe more natural) family of examples where the gap between TC and GC is unbounded.

REFERENCES

- [1] Z. Błaszczuk, J. Carrasquel-Vera, *Topological complexity and efficiency of motion planning algorithms*, Rev. Mat. Iberoamericana 34, Issue 4 (2018), 1679–1684.
- [2] D. Cohen and G. Pruidze, *Motion planning in tori*. Bull. Lond. Math. Soc. **40**, no. 2 (2008), 249–262.
- [3] D. Cohen and L. Vandembroucq, *Topological complexity of the Klein bottle*, J. Appl. and Comput. Topology 1 (2017) 199–213.
- [4] D. Davis, *An n -dimensional Klein bottle*, Proc. Edinburgh Math Society Section A (2019).
- [5] D. Davis, D. Recio-Mitter, *The geodesic complexity of n -dimensional Klein bottles* (2019), Preprint arXiv:1912.07411 .
- [6] A. Dranishnikov, *Topological complexity of wedges and covering maps*, Proc. Amer. Math. Soc. 142, no.12 (2014), 4365–4376.
- [7] M. Farber, *Topological complexity of motion planning*, Discrete Comput. Geom. 29 (2003), no. 2, 211–221.
- [8] M. Farber, *Topology of robot motion planning*, Morse theoretic methods in nonlinear analysis and in symplectic topology, NATO Sci. Ser. II Math. Phys. Chem., vol. 217, Springer, Dordrecht, 2006, pp. 185–230.
- [9] M. Farber, S. Tabachnikov and S. Yuzvinsky, *Topological robotics: motion planning in projective spaces*, Int. Math. Res. Not. (2003), no. 34, 1853–1870.
- [10] J. Gravesen, S. Markvorsen, R. Sinclair and M. Tanaka, *The Cut Locus of a Torus of Revolution*, Asian J. Math. 9 (1) (2005), 103–120.

- [11] Norio Iwase and Michihiro Sakai, *Erratum to “Topological complexity is a fibrewise L - S categor”* [*Topology Appl.* 157 (1) (2010) 10–21], *Topology Appl.* 159 (2012), no. 10-11, 2810–2813.
- [12] N. Iwase, M. Sakai and M. Tsutaya, *A short proof for $tc(K)=4$* , *Topology Appl.* 264 (2019), 167–174.
- [13] J. Lee, *Introduction to Riemannian Manifolds*, 2nd edition, Graduate Texts in Mathematics 176 (2018), Springer (1st edition 1997).

DEPARTMENT OF MATHEMATICS, LEHIGH UNIVERSITY, BETHLEHEM, PA 18015, USA
E-mail address: `dar318@lehigh.edu`